tvst

DOI: 10.1167/tvst.5.4.10

Article

A Novel Method of Quantitative Anterior Chamber Depth Estimation Using Temporal Perpendicular Digital Photography

Ehud Zamir[1,2,3], George Y.X. Kong[1,2], Tanya Kowalski[1], Michael Coote[1,2,3], and Ghee Soon Ang[1,2,3]

[1] Centre for Eye Research, Victoria, Australia
[2] The Royal Victorian Eye and Ear Hospital, Victoria, Australia
[3] Melbourne Eye Specialists, Victoria, Australia

Correspondence: Ehud Zamir, Centre for Eye Research Australia, 32 Gisborne Street, East Melbourne, Victoria 3002, Australia. e-mail: ezamir@unimelb.edu.au

Received: 26 January 2016
Accepted: 16 May 2016
Published: 29 July 2016

Keywords: anterior chamber depth; digital photography; photogrammetry; angle closure glaucoma

Citation: Zamir E, Kong GYX, Kowalski T, Coote M, Ang GS. A novel method of quantitative anterior chamber depth estimation using temporal perpendicular digital photography. Trans Vis Sci Tech. 2016; 5(4):10, doi:10.1167/tvst.5.4.10

Purpose: We hypothesize that: (1) Anterior chamber depth (ACD) is correlated with the relative anteroposterior position of the pupillary image, as viewed from the temporal side. (2) Such a correlation may be used as a simple quantitative tool for estimation of ACD.

Methods: Two hundred sixty-six phakic eyes had lateral digital photographs taken from the temporal side, perpendicular to the visual axis, and underwent optical biometry (Nidek AL scanner). The relative anteroposterior position of the pupillary image was expressed using the ratio between: (1) lateral photographic temporal limbus to pupil distance ("E") and (2) lateral photographic temporal limbus to cornea distance ("Z"). In the first chronological half of patients (Correlation Series), E:Z ratio (EZR) was correlated with optical biometric ACD. The correlation equation was then used to predict ACD in the second half of patients (Prediction Series) and compared to their biometric ACD for agreement analysis.

Results: A strong linear correlation was found between EZR and ACD, $R = -0.91$, $R^2 = 0.81$. Bland-Altman analysis showed good agreement between predicted ACD using this method and the optical biometric ACD. The mean error was −0.013 mm (range −0.377 to 0.336 mm), standard deviation 0.166 mm. The 95% limits of agreement were ±0.33 mm.

Conclusions: Lateral digital photography and EZR calculation is a novel method to quantitatively estimate ACD, requiring minimal equipment and training.

Translational Relevance: EZ ratio may be employed in screening for angle closure glaucoma. It may also be helpful in outpatient medical clinic settings, where doctors need to judge the safety of topical or systemic pupil-dilating medications versus their risk of triggering acute angle closure glaucoma. Similarly, non ophthalmologists may use it to estimate the likelihood of acute angle closure glaucoma in emergency presentations.

Introduction

Physical examination of the eye is usually carried out by an observer positioned in front of a patient in primary gaze. To obtain magnified, three-dimensional visual information about antero-posterior position of the ocular structures, an oblique slit lamp light beam is used, creating an optical section that improves the examiner's anatomical depth perception. The ability to shift the focal point of the slit lamp backward and forward also allows the examiner to qualitatively estimate the antero-posterior position of the objects.

Viewing the anterior segment from a direction perpendicular to the visual axis is not part of routine ocular examination. However, this viewing angle allows the examiner to see the profile of the corneal dome (hence Munson's sign in keratoconic eyes), as well as refractive lateral views of the iris, pupil, and anterior chamber. An intuitive, qualitative impression about the relative anteroposterior position of the pupil can be obtained from this angle of viewing. For

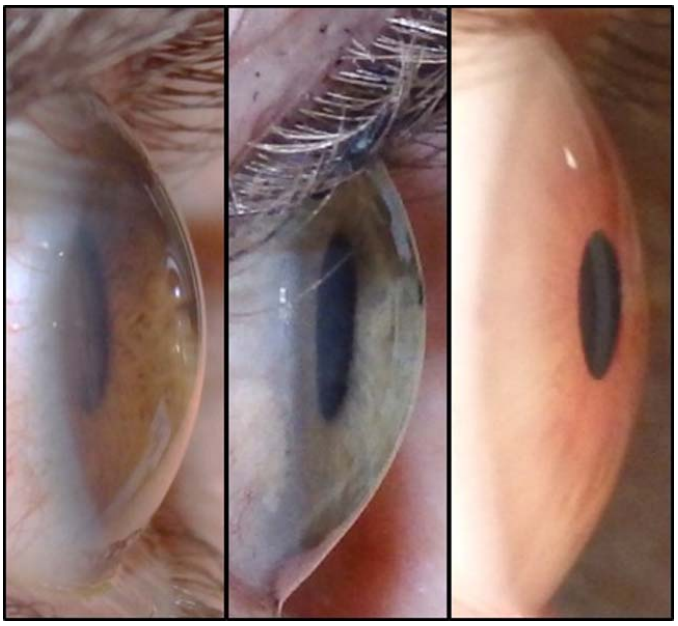

Figure 1. Lateral (temporal) perpendicular photographs of three different right eyes, showing an intuitively obvious, qualitative difference in the ACDs of these eyes. The eye on the left is pseudophakic, with a very deep anterior chamber. The middle eye is of moderately deep anterior chamber, and the one on the right has a shallow anterior chamber.

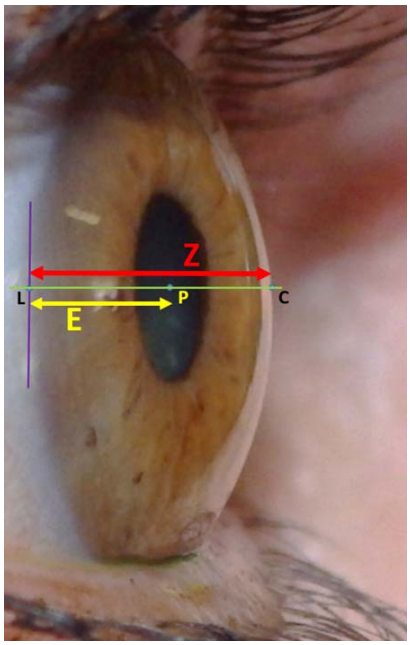

Figure 2. Lateral (temporal) perpendicular photograph of a right eye with a schematic outline of the photogrammetric method we used. The *cross* indicates the tangential limbus line (*vertical, purple*) and the limbus-pupil-cornea line (*horizontal, green*). The three *blue dots* mark the cardinal points, from left to right: Temporal limbal mark (L), mid pupil mark (P), and corneal mark (C). E, Lateral photographic temporal limbus to pupil distance; Z, Lateral photographic temporal limbus to cornea distance. The vACD is Z-E.

example, in eyes with very deep anterior chambers, the pupil may only be partially seen or not seen at all from the perpendicular position, if it is set too far posteriorly. Conversely, in eyes with shallow anterior chambers, the pupil appears anterior and closer to the cornea than to the temporal limbus (Fig. 1). We attempted to quantify this intuitive observation using digital photography and photogrammetry, in order to develop a simple clinical tool for estimating the ACD.

To create a quantitative measure of relative anteroposterior pupil position, we defined the following linear parameters as they apply to perpendicular lateral viewing and photography of the eye (Fig. 2): Z, the apparent antero-posterior distance from the temporal limbus to the corneal surface, and E, the apparent antero-posterior distance from the temporal limbus to the center of the pupillary image. Therefore, the more anterior the pupillary image is positioned along the limbus to cornea line, the larger the E:Z ratio (EZR).

We hypothesized that:

1. EZR is negatively correlated with anterior chamber depth (ACD).
2. This correlation can be used as a simple method for quantitative estimation of ACD.

We tested our hypothesis empirically and will present our findings, as well as the theoretical foundations of our empirical observations.

Methods

The study was approved by the Human Research and Ethics committee of the Royal Victorian Eye and Ear Hospital in Melbourne, Australia.

Study Subjects

We randomly recruited volunteering patients and their relatives from the Ear, Nose, and Throat Outpatient Clinic at the Royal Victorian Eye and Ear Hospital. The first half of subjects recruited, by chronological order, were assigned to the correlation series, while the second half was assigned to the agreement series. All subjects underwent lateral photography as well as automated ocular biometry performed by two authors (EZ and TK). Pseudophakic eyes were excluded from the study, as we found the biometer could not perform consistent ACD measurement in such eyes.

Volunteers were included if they were 18 years old or older. Eyes with previous penetrating corneal injury, incomplete biometry data, or with poor quality photographs were excluded from our analysis. Also excluded were eyes with lesions in the temporal limbal area, such as temporal pterygia, distorting or obstructing the view of the normal limbal anatomy.

Lateral Photography

Patients were instructed to look at a distant fixation target with one eye covered. The fixating eye was flash photographed using a digital camera (Canon 450D). Photographs were taken while aiming the camera from the temporal side, perpendicular to the visual axis and at the eye's height. Patients were instructed to open their eyes widely, in order to move the eyelashes away from the central anterior chamber and limbal structures. Bright ambient room lights were used in order to constrict the pupil and allow easier estimation of the center of the pupillary image in the photographs. Each eye was photographed three times and both eyes of each patient were photographed.

Optical Biometry (Scheimpflug Photography Based ACD Measurement)

We used the Nidek AL Optical Biometer (Nidek Co., Ltd., Aichi, Japan). Each eye underwent a biometric scan, using Scheimpflug photography to automatically record the ACD and central corneal thickness (CCT), and partial coherence interferometry to record axial length. keratometry and white-to-white distance (WTW).

For the purpose of this study, ACD was defined as aqueous depth (the distance between the anterior capsule of the crystalline lens and the corneal endothelium). In the Nidek data, this was derived from subtraction of CCT from the machine defined ACD, which includes the CCT.

Photogrammetric Analysis

Each photograph was viewed on a laptop computer. Photographs were analyzed by a final year medical student (TK). The area of interest was cropped using Irfanview (www.irfanview.com) and transferred to Microsoft PowerPoint. In each photograph, the temporal limbus was marked at the anterior surgical limbus (the posterior border of the blue-gray zone, on white sclera (Fig. 2).[1] A straight line, roughly tangential to the temporal limbal arc was traced freehand. Perpendicular to it, a line passing through the temporal limbus and the estimated center of the pupillary image was drawn and extended anteriorly to intersect with the cornea. A corneal mark was placed at the anterior corneal intersection point (Fig. 2).

A pixel ruler (Screen Ruler V.1.0.1a, caveworks.net) was used for measuring pixel distances in each image. The pixel distance between L and C was called Z, and the pixel distance between L and P was called E. The distance P to C is the virtual ACD (vACD). The ratio between E and Z was calculated and recorded. Three photographs of each eye were measured separately. The EZRs from these three photographs were averaged and the means were used for our analyses.

Statistical Analysis

Patient biometric and photogrammetric data were analyzed using Microsoft Excel as follows:

1. To test our first hypothesis, the chronological first half of eyes were labelled "Correlation Series." Pearson's coefficient (R) was calculated for the correlation between EZR and the biometric ACD in this series, using Microsoft Excel. The line of best fit for the scatter diagram of this correlation series was generated and its linear equation was recorded.
2. To test our second hypothesis, the correlation equation derived from the Correlation Series was used to predict ACD in the remaining half (the Prediction Series). This prediction was then compared to the biometric ACD of those eyes. Scatter plots of the Prediction Series were generated, showing predicted (x axis) versus biometric ACD (y axis), and Bland-Altman agreement analysis (MedCalc, MedCalc Software, Ostend, Belgium) was used to show the agreement between predicted ACD and biometric ACD measurement.
3. Intraclass correlation coefficient (ICC) was used for the assessment of intra- and interobserver reliability in measurement of EZR. ICCs were calculated using SPSS (version 16.0, SPSS, Inc., Chicago, IL) with Two-Way Mixed model set to examine absolute agreement.

Results

A total of 266 eyes of 146 individuals were included in the study. Twelve eyes were excluded from the analysis due to poor photographic quality,

Table. Patient Biometric Characteristics

	Correlation Series	Prediction Series
N	132 eyes (74 individuals)	134 eyes (72 individuals)
Age (mean ± SD, range), y	59.19 ± 14.94, 23–84	53.82 ± 15.74, 24–92
M:F ratio	29:45	30:42
Biometric ACD excluding CCT (mean ± SD, range), mm	2.62 ± 0.38, 1.66–3.6	2.53 ± 0.39, 1.67–3.68
White to white diameter (mean ± SD, range), mm	11.93 ± 0.45, 9.8–13.0	11.92 ± 0.46, 9.6–13.1
Mean corneal radius (mean ± SD, range), mm	7.74 ± 0.26, 7.11–8.39	7.79 ± 0.30, 6.88–8.98
Axial length (mean ± SD, range), mm	23.32 ± 1.01, 20.31–27.39	23.28 ± 1.09, 20.18–27.53

and eight eyes were excluded due to poorly defined limbal landmarks. Patient biometric characteristics are presented in the Table.

Correlation Between EZR and Biometric ACD

In the Correlation Series, a strong negative correlation was found between EZR and biometric ACD. Pearson's correlation coefficient R was −0.90, R^2 was 0.81 and the linear equation of the line of best fit was: ACD = −3.273EZR + 4.18 (Fig. 3).

EZR as an ACD Estimation Tool: Agreement Between EZR-Predicted and Biometric ACD

The above empirically derived correlation equation was used as an instrument to predict the ACD in each of the 132 eyes that were randomly assigned to the Prediction Series, thereby testing our second hypothesis. That prediction was then compared to the biometric ACD for agreement analysis. The difference between the two values (Predicted ACD) − (Biometric ACD) was defined as the error for that eye. The mean error was −0.013 mm (range −0.377 to +0.336 mm). The standard deviation of the errors was 0.166 mm. Given the mean ACD in this series was 2.53 mm, the coefficient of variation (relative standard deviation) was 6.5%.

Figure 4A demonstrates the scatter of predicted versus biometric ACD values for the 134 eyes in the agreement series. Figure 4B is a Bland-Altman plot of the agreement between predicted and biometric ACD. We regarded biometric ACD as a gold standard benchmark. We therefore used it, rather than the mean between predicted and biometric ACD, as the x axis in Figure 4B.

Repeatability and Reproducibility

Two observers were responsible for obtaining measurements from digital images in our study (EZ and TK). Intraobserver reliability was examined for each observers using a random sample of 50 eyes from our study. Each observer marked the cardinal landmarks and measured the EZR in three different photos per eye in their respective sample, and the intraobserver reliability was assessed with ICC. Observer 1 (EZ) showed high degree of reliability with average ICC of 0.995 (95% confident interval: 0.992–0.997) and similarly Observer 2 (TK) had ICC of 0.999 (95% confident interval: 0.996–0.999). These values demonstrate that our method is reliably repeatable within the same observer.

Interobserver reliability was assessed with another randomly selected sample of 20 eyes from our study. Each observer independently graded three photographs per each of the 20 eyes and the average EZRs were compared between the two observers. The average ICC was 0.9831, thus demonstrating that there is high level of concordance between the two observers.

Discussion

Our goal in the work presented here was to develop a simple method for quantitative estimation

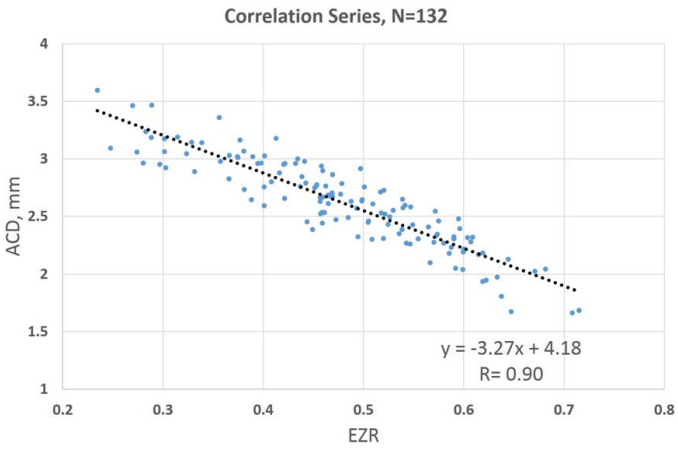

Figure 3. EZ ratios scatter plot against biometric ACD (Correlation Series, $N = 132$ eyes) showing a strong negative linear correlation.

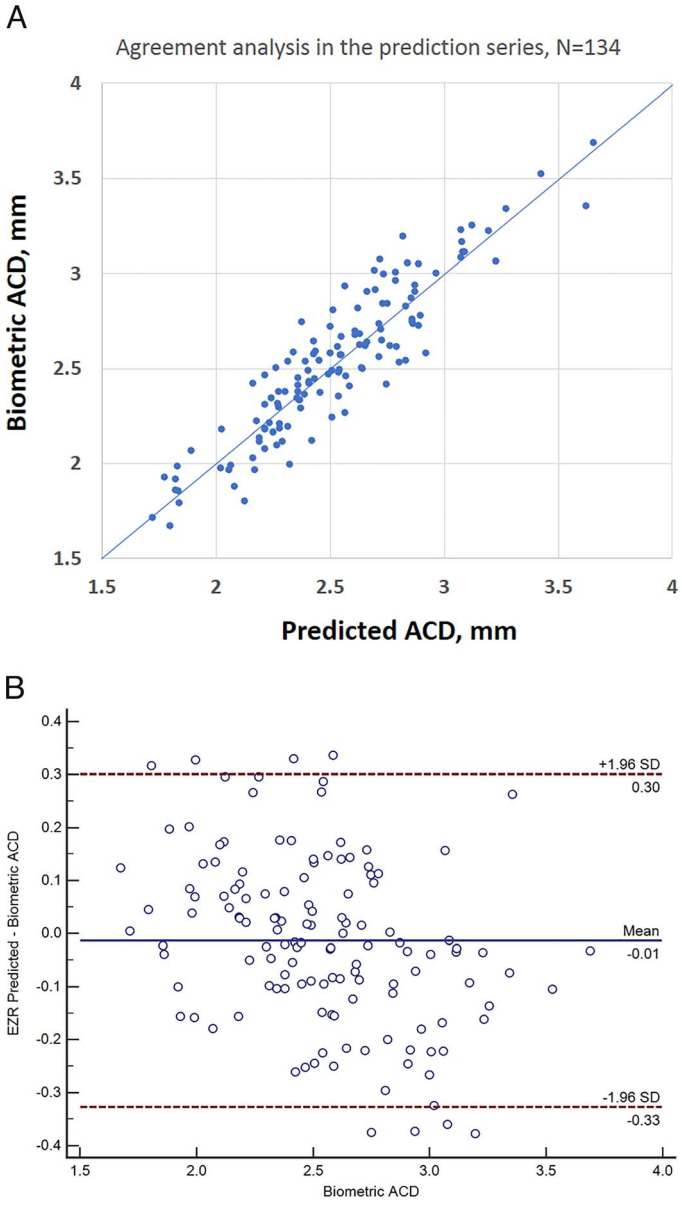

Figure 4. Agreement analysis. (A) Agreement between the predicted and biometric ACD (Prediction Series, $N = 173$ eyes). The line represents perfect agreement. (B) Bland-Altman agreement analysis between the predicted and biometric ACD (Prediction Series, $N = 173$ eyes). The error (Predicted minus biometric ACD) is represented on the Y axis.

of the central ACD, to be used by clinicians who do not have access to ophthalmic equipment and/or who have limited ophthalmic examination skills.

We attempted to quantify the observation that in eyes with deep anterior chambers the pupillary image is relatively posterior and vice versa, when observing perpendicularly to the visual axis. The geometric optical explanation for this phenomenon is shown in Figure 5.

Our method evolved in few stages. Firstly, we hypothesized a correlation existed between the vACD and the real ACD. Indeed, as derived from our optical discussion in Appendix 1 about the corneal refractive effect, there is a theoretical linear correlation between these variables: ACD = 0.96 vACD + 0.9 (Appendix 1). According to this theoretical equation, the anterior chamber is deeper than its virtual image (vACD) by an average of 0.88 to 0.72 mm for the ACD range of 1.5 to 5 mm, respectively, when viewed from the lateral perpendicular position.

Estimating real ACD based on such a correlation requires calibrated photography in order to measure vACD in mm. However, calibrated photography for direct measurement of vACD is relatively cumbersome. It requires knowledge of the object distance, which is not a common feature in digital cameras or smartphones at present. In order to simplify the method, we thought of using a proportion rather than an absolute length. We chose the denominator of that proportion to be the anteroposterior distance between the temporal limbus and the front of the cornea (Z). We hypothesized Z was an approximately constant value, which may serve as a photographic "scale" in each photograph. Conceptually, this is similar to the use of the ratio between the corneal thickness and the aqueous band width when performing a van Herick's assessment of the peripheral anterior chamber angle.[2] There, too, the basis for the estimate is an approximately constant corneal thickness that is used as a comparator.

Z may be shown to be dependent on R and WTW, as shown in Figure 6, with the equation $Z = R - \sqrt{R^2 - \frac{WTW^2}{4}}$. Using our biometrically obtained values for R and WTW for each eye in our study, this calculation yielded Z values with a mean of 2.8 mm and a narrow normal distribution (Fig. 7). We therefore chose EZR as a candidate measure for correlation with ACD. As shown in Appendix 1, the theoretical relationship between EZR and ACD is approximately linear. Both the theoretical and empirically derived correlations support hypothesis 1. We also showed that the empirically derived correlation can be used as an instrument to estimate the ACD with clinically acceptable accuracy, supporting hypothesis 2. The error of this estimate, compared to gold standard ACD measurement, had a 95% limit of agreement of ± 0.33 mm, and the error's coefficient of variation was less than 7% of the average ACD in our series. This magnitude of agreement is comparable with the limits of agree-

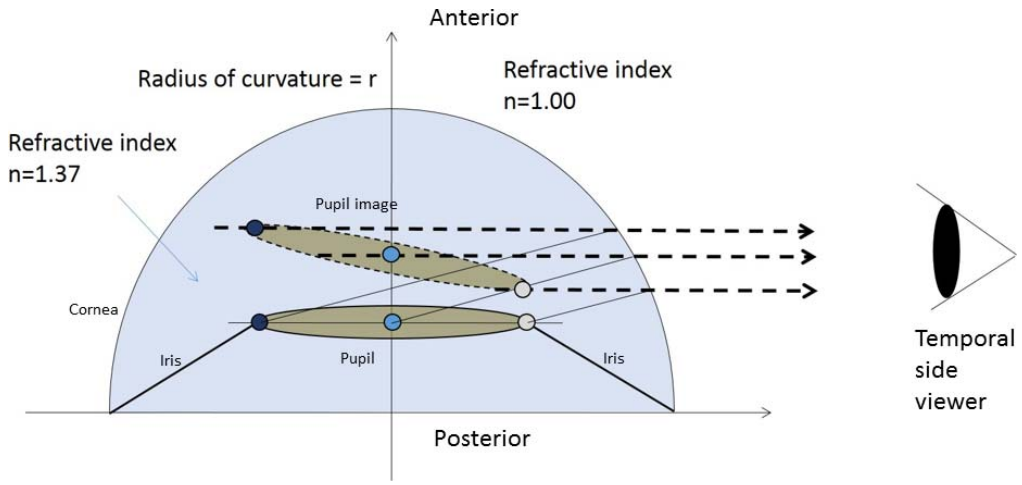

Figure 5. Corneal-Aqueous refraction results in the formation of a virtual, oblique pupil image anteriorly to the true pupil plane. The further the object is from the viewer, the more anteriorly is its image displaced.

ment between established automated methods for ACD measurement, such as partial coherence laser interferometry (IOL Master), scanning peripheral anterior chamber analyser and anterior segment OCT: In a study by Lavanya et al.,[3] these methods demonstrated 95% limits of agreement of 0.4 to 0.5 mm in ACD measurements when analyzed for agreement between them.

There were several potential sources for error in our method. We will briefly discuss the technical and then the theoretical sources of error:

Perpendicularity of the camera lens to the visual axis was subjective and intuitive, rather than based on accurate geometrical positioning. This inevitably introduced rotation to some of the images taken, leading to a potential error in measuring EZR. The same error can be introduced by any source of inaccuracy in the patient's fixation, and by the variability of angle Kappa. In the process of analyzing the photograph, the cardinal anatomical points L, P, and C were manually determined. Although this manual process was robust, as evident by high repeatability and reproducibility, we found that accurately determining the limbal point on the photographs was sometimes difficult, especially in patients with arcus senilis or indistinct limbal landmarks.

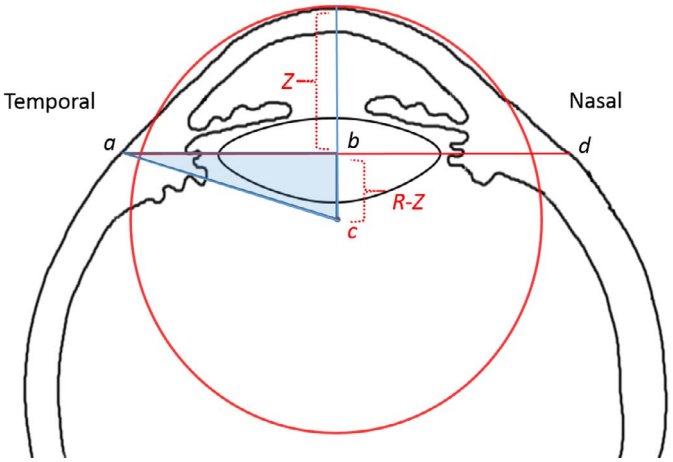

Figure 6. Mid-axial section of a schematic eye. The shaded triangle abc will be considered, where a is the temporal limbus, d is the nasal limbus, b is the midpoint of ad, and c is the center of the corneal "sphere." In that triangle, $ab = \text{WTW} / 2$, $ac = R$, the corneal radius, and $bc = R - Z$. Using Pythagoras theorem: $R^2 = ab^2 + (R - Z)^2$, $R - Z = \sqrt{R^2 - ab^2}$, therefore $Z = R - \sqrt{R^2 - \frac{WTW^2}{4}}$.

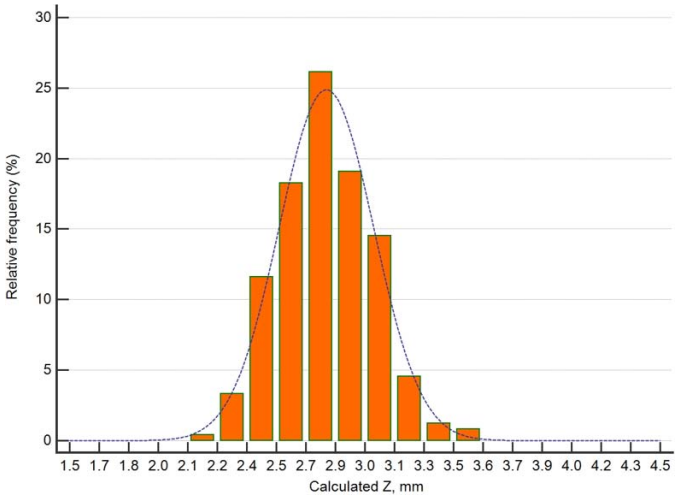

Figure 7. A histogram showing the distribution of calculated Z in our patients, using the expression $Z = R - \sqrt{R^2 - \frac{WTW^2}{4}}$ to calculate Z in each eye, $N = 266$.

Our theoretical model makes several assumptions and approximations, including a spherical cornea of a given curvature of 7.8 mm, an equal refractive index of 1.37 to the cornea and aqueous humor, and a far enough photographic distance to result in parallel light rays from the eye entering the camera lens. In reality, the photographic distortion introduced by the corneal refraction varies with corneal curvature,[4,5] which in turn also changes the value of Z. We assumed both of these parameters to be constant in reaching our theoretical equations. Our observational data show that despite the above approximations and sources of error, our predicted ACD values were of clinically acceptable accuracy in a large series of eyes.

The accuracy of this method may be further improved by its users. For instance, in populations where the biometric features differ significantly to ours, adjustments to our equations may be made as needed.

The main strength of the EZR method is the ease of obtaining a quantitative measure of ACD with minimal equipment and training. However, we used a multistep process, starting with image acquisition on a camera, then photogrammetric measurements on a computer. This multistep process is time consuming and more work is required to sophisticate it to a single step, automated process.

Unlike slit lamp based methods, the EZR method requires little training and knowledge about the eye, and no special equipment. As such it may be used by a wide potential audience, including doctors of various specialties, optometrists, ophthalmic technicians, nurses, and even the lay public.

Shallow ACD is one of the cardinal risk factors in the pathogenesis of angle closure glaucoma.[6–8] A simple tool for estimating ACD may assist in identifying patients at risk or excluding the risk of angle closure glaucoma, either as a screening tool or on an individual patient basis. Assessment of the risk of inducing acute angle closure is also relevant for non ophthalmologists prescribing anticholinergics, antiemetics, antidepressants, and various anaesthetic agents that may trigger acute angle closure in susceptible patients. ACD is sensitive but not specific enough for screening for angle closure glaucoma on its own, but its high sensitivity and high negative predictive value mean that if an ACD is deeper than a threshold level, the risk of ACG is low.[7–11] This makes it useful when angle closure glaucoma needs to be ruled out, such as in the hands of general physicians treating patients with an acutely red eye.

We are not aware of other quantitative methods for estimation of the ACD without ophthalmic equipment. The flashlight test is a simple method for estimating the anterior chamber angle and depth.[12] However, it is subjective and qualitative. In contrast, our method is objective, photography-based (therefore also allowing re-examination of the data or remote analysis) and quantitative.

In conclusion, we describe a novel anterior segment anatomical proportion, EZR, which may be calculated using a simple digital camera and minimal computation capabilities present on most smartphones. We brought data showing that it can be used to derive a quantitative estimate of ACD in a simple process that requires minimal skill.

Acknowledgments

We thank Richard Smallwood and Matthew Ayres from the Medical Photography Department at the Royal Victorian Eye and Ear Hospital for their professional help, advice, and support during this project. We also thank Ido Zamir, Yael Zamir, and Keren Zamir for their help in the development of the EZ ratio concept, and Designs for Vision, for volunteering the Nidek AL Scan for the experiment.

Disclosure: **E. Zamir**, None; **G.Y.X. Kong**, None; **T. Kowalski**, None; **M. Coote**, None; **G.S. Ang**, None

References

1. Van Buskirk EM. The anatomy of the limbus. *Eye (Lond)*. 1989;3:101–108.
2. Van Herick W, Shaffer RN, Schwartz A. Estimation of width of angle of anterior chamber. Incidence and significance of the narrow angle. *Am J Ophthalmol*. 1969;68:626–629.
3. Lavanya R, Teo L, Friedman DS, et al. Comparison of anterior chamber depth measurements using the IOLMaster, scanning peripheral anterior chamber depth analyser, and anterior segment optical coherence tomography. *Br J Ophthalmol*. 2007;91:1023–1026.
4. Goldmann H. Eine methode zur volumbestimmung der vorderkammer des lebenden menschen. *Ophthalmologica*. 1941;102:107.

5. Heim M. Photografishce bestimmung der tiefe und des volumens der menschlichen vorderkammer. *Ophthalmologica*. 1941;102:193.
6. Aung T, Nolan WP, Machin D, et al. Anterior chamber depth and the risk of primary angle closure in 2 East Asian populations. *Arch Ophthalmol*. 2005;123:527–532.
7. Tornquist R. Shallow anterior chamber in acute glaucoma: a clinical and genetic study. *Acta Ophthalmol Suppl*. 1953;39:1–74.
8. Tornquist R. Chamber depth in primary acute glaucoma. *Br J Ophthalmol*. 1956;40:421–429.
9. Congdon NG, Youlin Q, Quigley H, et al. Biometry and primary angle-closure glaucoma among Chinese, white, and black populations. *Ophthalmology*. 1997;104:1489–1495.
10. Devereux JG, Foster PJ, Baasanhu J, et al. Anterior chamber depth measurement as a screening tool for primary angle-closure glaucoma in an East Asian population. *Arch Ophthalmol*. 2000;118:257–263.
11. Zhang Y, Li SZ, Li L, Thomas R, Wang NL. The Handan Eye Study: comparison of screening methods for primary angle closure suspects in a rural Chinese population. *Ophthalmic Epidemiol*. 2014;21:268–275.
12. Thomas R, George T, Braganza A, Muliyil J. The flashlight test and van Herick's test are poor predictors for occludable angles. *Aust N Z J Ophthalmol*. 1996;24:251–256.